OPERATIONAL EXPERIENCE AT LCLS*

H. Loos†, SLAC National Accelerator Laboratory, Menlo Park, CA 94025, U.S.A.

Abstract

The Linac Coherent Light Source (LCLS) X-ray FEL has been operational since 2009 and is delivering soft and hard x-rays to users now in the 4th user run. Reliable operation to deliver x-rays to users, quick machine turn on after shutdowns, and fast configuration changes for the wide range of user requests are particularly important for a facility serving a single user at a time. This talk will discuss procedures to set-up and optimize the accelerator and FEL x-ray beam for user operation. The emphasis will be on the most relevant diagnostics and tuning elements as well as the experience with feedback systems and high level support software to automate FEL operation.

INTRODUCTION

The Linac Coherent Light Source (LCLS) [1] is the first FEL operating at soft and hard X-ray wavelengths down to 1.2 Å. After first lasing was achieved in April 2009 [2], beam operation for user experiments is now in its fourth run. The FEL consists of a high-brightness photo-injector followed by the last 1 km of the 2-mile SLAC linac modified with 2 bunch compressors, a beam transport line and the 130 m long undulator divided into 33 segments. The X-ray diagnostics follow in the Front End Enclosure (FEE) together with the mirror system for soft-and hard X-ray transport lines to the Near and Far Experimental Halls (NEH and FEH), each housing three experimental stations. Of the six instruments, four are now in operation (AMO, SXR, XPP, CXI), one is in commissioning state (XCS), and one is still under construction (MEC) and will be operational in 2012. A list of the main LCLS parameters can be found in Table 1.

Table 1: LCLS Parameters

	Baseline	Achieved
Repetition rate (Hz)	120	120
Electron energy (GeV)	$4.3 - 13.6$	$3.3 - 15.4$
Bunch charge (pC)	200&1000	$20 - 250$
Emittance norm. (μm)	1.2	$0.13 - 0.5$
X-ray energy (keV)	$0.83 - 8.3$	$0.48 - 10.5$
X-ray pulse energy (mJ)	< 2	< 4.7
X-ray pulse length (mJ)	230	$< 5 - 500$

The following sections will describe the operation of LCLS as a user facility and the necessary tasks and tools to setup and tune the accelerator to the range of parameters requested by the users.

USER OPERATION

The availability of the LCLS beam in terms of actual vs. planned beam operation is shown in Fig. 1 has been about 97% for the three completed user runs from October 2009 to March 2011. The photon beam availabilityfor the three runs is now getting close to the set LCLS operation goal of 95%.

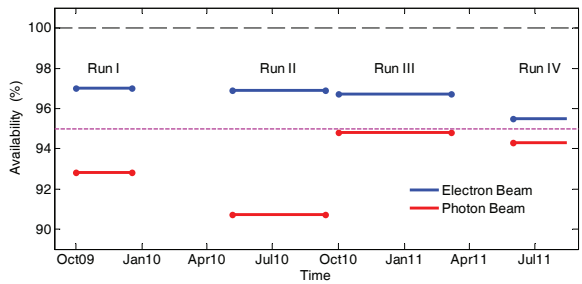

Figure 1: Electron and photon beam availability for LCLS for user runs I to IV. The set goal of 95% is indicated by the dotted line.

Beam operation for LCLS is divided on a weekly basis in normally 5 days of X-ray delivery to user experiments and two days midweek for machine development and maintenance. Usually the X-ray beam is switched between two or three different user experiments on a two 12 h shift per day schedule. Every two weeks the accelerator is shut down for an entire shift for necessary maintenance and repair work followed by a shift to recover beam operation and to setup accelerator configurations needed for the different user experiments scheduled.

LCLS Parameter Range

The main parameters of LCLS to be setup for user experiments are the photon wavelength, photon pulse length, and the bunch charge mode of the accelerator, with the respective ranges listed in Table 1. A detailed layout of the LCLS is shown in Fig. 2 with the gun/injector area, the main acceleration sections (L0-L3) and bunch compressors (BC1, BC2), a beam transport line (DL2) and the undulator, and the photon diagnostic and X-ray mirror system. The locations of the main electron beam diagnostics [3] with OTR screens, wire scanners, transverse deflecting cavities (TCAV) and bunch length monitors is also indicated.

* Work supported by US DOE contract DE-AC02-76SF00515.
† loos@slac.stanford.edu

ISBN 978-3-95450-117-5

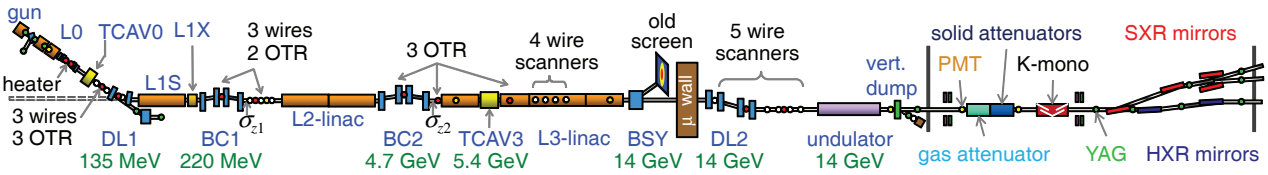

Figure 2: Layout of the LCLS accelerator, electron beam diagnostics, and photon diagnostic and distribution systems.

With a fixed-gap undulator, the photon wavelength has to be adjusted by changing the electron beam energy, which is done by keeping the energy profile up to the second bunch compressor at 4.7 GeV and then selecting an adequate number of acceleration sections in the L3 linac to either decelerate to energies down to 3.3 GeV or accelerate to up to 15.4 GeV. Fine adjustment of the final beam energy is achieved by setting parts of the L3 linac to opposing phases.

The photon pulse length is set by the electron bunch length which is selected by the peak current set point after BC2 of the longitudinal feedback in the control system. This actually sets the proper phase and amplitude of the L2 linac to get the desired chirp for the final bunch compression in BC2.

The LCLS can be operated in two main charge modes, the nominal high charge mode at 150 or 250 pC enabling FEL operation in the $50 - 500$ fs pulse length range and a low charge mode at 20 or 40 pC [4] with about 10% of the normal X-ray pulse energy, which can deliver ultra-short pulses of less than 5 fs (estimated). Switching between the two charge modes requires changes to the cathode laser spot size, the injector RF phase and lattice setup, and some minor tuning of the main linac.

The main driver for tuning and setup changes of the accelerator is the range of requests from the user experiments for different X-ray beam parameters, however, occasional tuning is also required from changes to the input conditions of the electron beam in the injector, namely the profile of the UV photo-injector laser and the quantum efficiency profile of the cathode itself. In order to achieve reproducible results from the machine tuning, clearly defined procedures have to be in place for the initial machine setup after a change in the X-ray parameters. The subsequent fine tuning of the FEL performance should then only use a limited subset of the available knobs to stay within design conditions for as much of the machine as possible. Another important aspect is the availability of feedback loops and feed-forward algorithms to decouple different accelerator parameters like beam energy, bunch length, and beam orbit at various locations in the machine from each other. The efficiency and timeliness of the machine setup is further enhanced by software automation of many measurements and setup procedures.

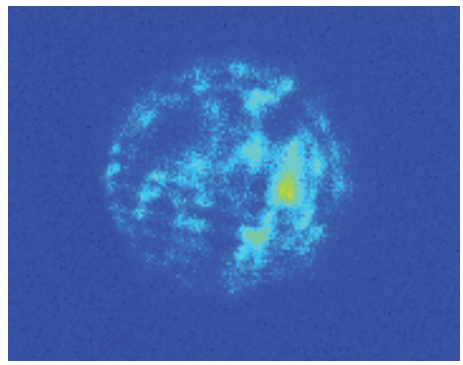

Figure 3: Cathode beam emission imaged on a downstream YAG screen. The diameter of the beam is about 5.5 mm, corresponding to a UV-laser diameter of 1.2 mm on the cathode.

Injector Tuning

Tuning of the LCLS injector [5] beam emittance is mostly necessary during a change of the bunch charge mode, and also when the cathode emission pattern as shown in Fig. 3 changes after a cathode cleaning procedure or when a different location on the cathode is illuminated. The emittance is measured using the quadrupole scan method on an OTR screen located downstream after the L0 linac and the deflecting cavity at 135 MeV. The measuring software is fully automated (Fig. 4) and can in turn be invoked by other scripts to measure the beam emittance as a function of any other accelerator parameter.

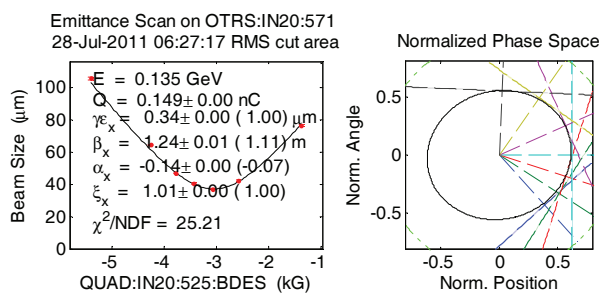

Figure 4: Results from a fully automated quadrupole emittance scan on an injector OTR screen for the horizontal plane. Data for the simultaneously acquired vertical plane is not shown.

This is for instance used to vary the gun solenoid

ISBN 978-3-95450-117-5

strength to find the proper setting to minimize both horizontal and vertical beam emittance. Additionally is is necessary to also vary both the normal and skew quadrupoles embedded in the gun solenoid to remove the effect of asymmetries between the horizontal and vertical planes in the laser distribution on the beam emittance. The two parameter scan shown in Fig. 5 required 49 emittance measurements and took less than an hour.

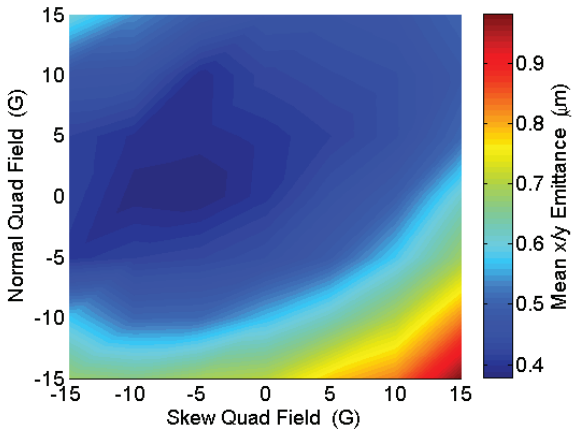

Figure 5: Two parameter scan of the injector emittance varying the normal and skew quadrupole in the gun solenoid.

The tuning of longitudinal beam properties is enabled by the transverse deflecting cavity (TCAV0) in the injector and the downstream OTR screen. The calibration of the vertically deflecting cavity is done by software which records the beam position on the screen while scanning the cavity phase. A measurement of the vertical beam size at the two RF-zero crossings and with no deflection then enables an automated and fast bunch length measurement. Combining the deflecting cavity with the emittance measurement, the horizontal emittance of individual time slices can be obtained as shown in Fig. 6. The uniformity of the slice emittance and the matching of the slices to the design lattice along the duration of the bunch can be monitored in this way.

The longitudinal phase space can be observed with the streaked beam sent into the 135 MeV injector spectrometer. The temporal overlap of the laser heater beam with the electron beam can thus be optimized by scanning the time delay of the laser beam with respect to the electron beam and measuring the increase in energy spread of the central horizontal slice.

Feedback systems

Tuning and stable operation of the LCLS electron beam is greatly facilitated by the transverse and longitudinal feedback systems [6]. A total of 9 transverse feedbacks for the electron beam and additional loops for the photocathode and heater laser have been implemented. For the electron beam they are separated into individual loops for each

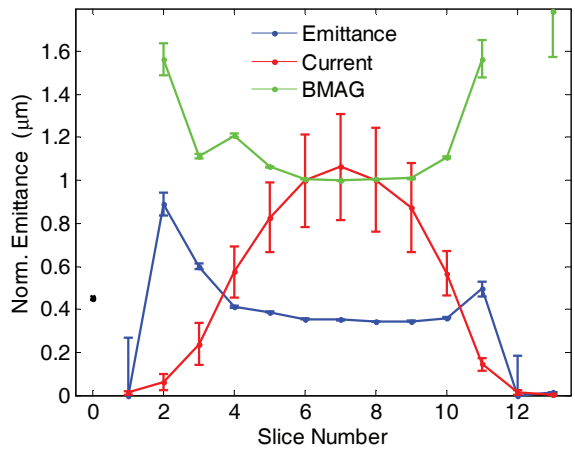

Figure 6: Injector horizontal slice emittance from combining a quadrupole emittance scan with streaking by the transverse deflecting cavity. The current profile represents a 460 μm (rms) long electron bunch. The dimensionless BMAG [5] quantifies the mismatch of the measured phase space to the design Twiss parameters with the lowest value of 1 for the matched case.

accelerating section (L0 - L3) and additional feedbacks for the beam transport line upstream of the undulator and for the undulator orbit itself. The feedbacks are independent loops and decoupled by operating them with different response times and loop gains.

The presently used implementation for the longitudinal feedback consists of independent loops for accelerating sections L0 - L3. For the L0 and L3 sections only an energy feedback exists which controls the effective accelerating voltage of the section based on an energy measurement. The two linac sections L1 and L2 upstream of the bunch compressors BC1 and BC2 have both effective voltage and phase controlled via inputs from energy and bunch length measurements. Both the energy and bunch length regulation are decoupled from each other by using virtual orthogonal actuators for energy gain and chirp of the respective section which then get translated into actual phase settings for the individual accelerating structures within that section. Additionally a fast feedback network [7] has been implemented to set individual RF parameters for the two 60 Hz AC power line cycles used at 120 Hz operation, so that differences in the klystron amplitudes and phases between the two cycles can be eliminated by the feedback loops.

The set points for all transverse and longitudinal feedbacks are accessible to other high level applications through the LCLS control system and can therefore be used to optimize the electron beam and FEL performance by varying parameters of individual parts of the accelerator while keeping the conditions in the rest of the machine constant.

ISBN 978-3-95450-117-5

Linac Tuning

Regular beam based measurements of the RF phase of all the accelerating structures are necessary for the longitudinal feedback to operate correctly and to obtain a proper calculation of the energy profile along the machine. Such phase scans are usually done daily for the main injector and linac accelerator sections by an automated script which adjusts the respective phase offsets. An example is shown in Fig. 7.

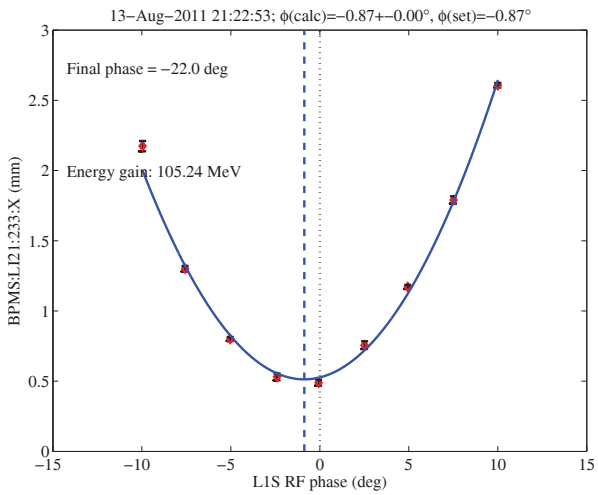

Figure 7: Phase scan result for the L1 accelerator section measuring the energy gain with a BPM in the downstream bunch compressor. The observed 1 ° phase change since the last measurement was automatically corrected.

Emittance measurements in the main linac up to the undulator are done with wire scanners with which only projected values can be measured as seen in Fig. 8. Tuning of the emittance at the three measurement stations after BC1, BC2, and upstream of the undulator involves matching to the design lattice at each location. Furthermore the beam position through the small X-band cavity and the orbit launch conditions into the L2 and L3 linac are varied with the set points of the feedback system to minimize the effect of wake fields and limit the emittance growth through out the machine.

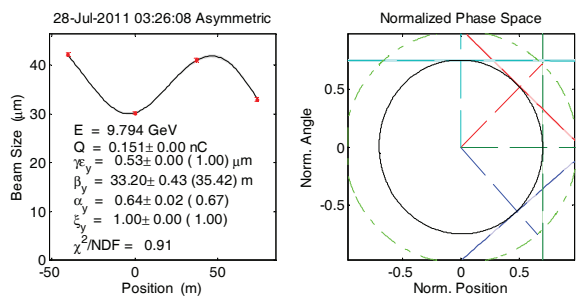

Figure 8: Emittance measurement of the vertical plane in the L3 linac using 4 wire scanners at 45° phase advance.

Undulator Operation

Efficient SASE operation of LCLS at the shortest wavelengths requires an orbit straightness within the undulator of only a few μm. Beam-based alignment of the undulator sections [8] is achieved to initially setup and then maintain this straightness requirement. Additionally an independent alignment diagnostic system (ADS) is used to monitor daily and long term drift of the undulator position [9].

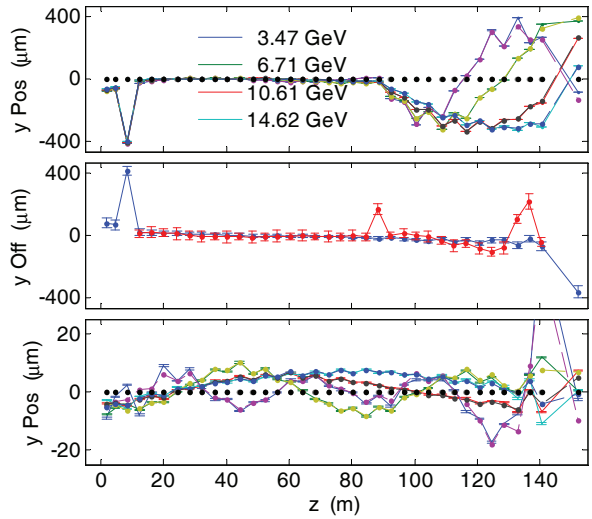

Figure 9: Beam-based alignment procedure of the undulator. Top part are average undulator orbits for four different beam energies; middle part are fitted quadrupole (red) and BPM offsets (blue); bottom part shows final orbits after three iterations.

From operational experience it is sufficient to perform the beam-based alignment every two weeks to address long term drifts, orbit changes from replaced undulator segments, and drifts in the RF cavity beam position monitor electronics. The procedure itself is semi-automatic and requires changing the beam energy to usually four different values covering the entire LCLS energy range and obtaining average beam orbits for each energy [10].

An example is shown in Fig. 9. The initial beam orbits in the vertical plane are on top exhibiting a strong kick from a previously replaced undulator segment. A fit of the entire data set (see center of figure) to quadrupole offsets, BPM offsets and orbit launch conditions into the undulator is then used to find the dispersion free orbit through the undulator. The fitted offsets are then used to correct the quadrupole positions by moving the supporting undulator girders and to correct the BPM positions in the controls software. After a few iterations in the procedure a dispersion free orbit can be achieved with rms deviations of only a few μm as shown in the bottom of Fig. 9. The entire procedures is usually completed within a few hours.

The K-value of the fixed gap LCLS undulators can be changed over a small range due to the wedged poles by horizontally translating the entire undulator segment, which in

ISBN 978-3-95450-117-5

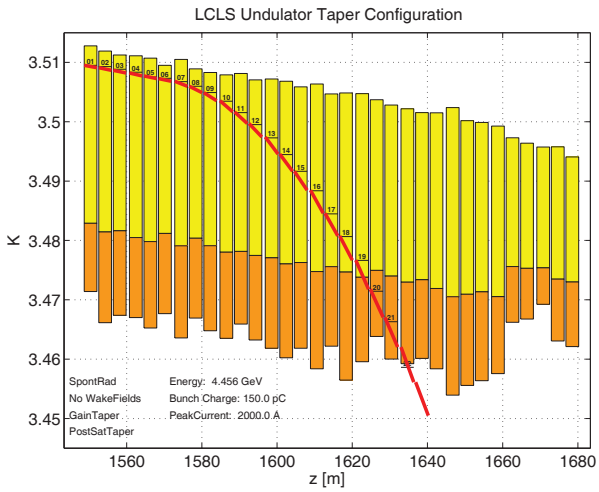

Figure 10: Software for taper setting. The first 6 undulators have a linear taper function applied while the next 17 also have an exponential taper functions added. The remaining segments are retracted.

turn can also be completely retracted. The K-values of the undulator segments are preset to a linear taper along the 33 undulator segments only compensating for energy loss from wakefields and spontaneous radiation. A high level software is used to set the taper based on combinations of a linear function for linear gain regime and an exponential function for the saturation regime. A sample taper setting by the software is shown in Fig. 10 for soft X-ray operation where only 23 of the 33 undulators where used to reach saturation. The parameters of the taper functions can be set by any other application and also automatically be applied by the taper software to enable optimization of the X-ray pulse energy by varying the taper parameters [11].

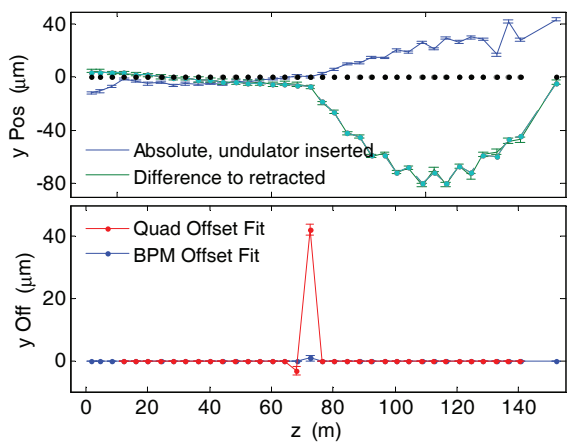

Figure 11: Absolute and difference orbit between inserted and retracted undulator segment 16 and fit results for adjacent quadrupole and BPM offsets.

The horizontal translation of the undulators to set different K-values or to retract them from the beam pipe affects the undulator orbit through variations of the undulator field integrals and in case of full retraction, through the exposed earth magnetic field and change in girder position from the weight shift. The first field integral measured for each undulator in the magnetic measurement lab can be compared with a beam-based measurement. The undulator is translated in steps and the first field integral is then obtained from the orbit kick at the undulator position with respect to the reference orbit at the center position. A similar procedure is done for the difference orbit between the inserted and retracted undulator position as shown in Fig. 11 for undulator 16, in this case offsets for the upstream and downstream quadrupole and downstream BPM position are obtained to account for the girder position change.

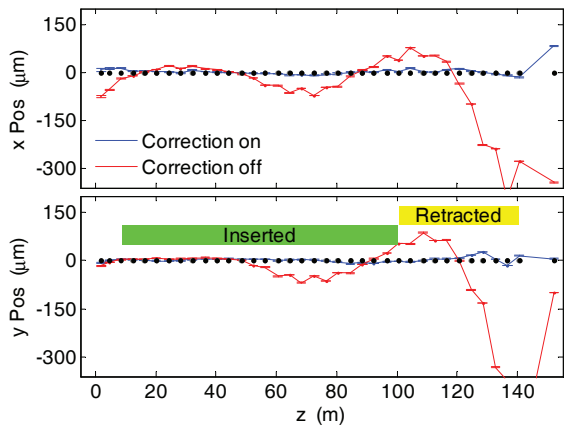

Figure 12: Effect of undulator field integral correction scheme. Blue orbit is with the feed-forward turned on, red orbit without feed-forward.

The orbit distortions due to a change in the undulator taper configuration can be of the order of several 100 μm. A feed-forward has been implemented in the undulator control system to automatically compensate both the changes in the field integral from undulator translation and the orbit kicks from retracting undulators using the steering coils embedded in the undulator quadrupoles. The effect of the correction scheme can be seen in Fig. 12 where with no correction the orbit can deviate by a few hundred μm whereas with the automatic correction turned on the orbit remains flat. The effect is largest in the latter part of the undulator where the last 10 segments were retracted. This correction scheme greatly facilitates changes in the undulator configuration needed for different photon energies and enables fast scans of taper parameters to optimize the FEL pulse energy without performance degradation from orbit distortions.

X-Ray Energy

The absolute value of the X-ray pulse energy in LCLS is obtained from a measurement of the electron energy loss induced by the FEL process. The energy loss is determined from the difference in the beam energy measured upstream in DL2 and downstream of the undulator in the main beam

ISBN 978-3-95450-117-5

dump. This energy loss also includes losses due to wake fields and spontaneous radiation and the FEL contribution is determined by inducing an orbit oscillation in the undulator to inhibit the FEL process. Figure 13 shows an energy loss scan with a simultaneous recording of photomultiplier signals from a gas detector in the FEE X-ray diagnostic area which is used to calibrate the gas detector against the absolute pulse energy measurement from the electron beam. Each time the photon energy is changed, this calibration has to be repeated to account for the wavelength dependency of the gas detectors.

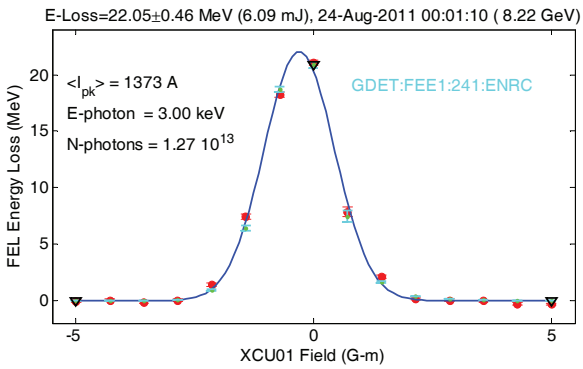

Figure 13: FEL energy loss scan by varying a steering coil at the beginning of the undulator to suppress the FEL process. Measured energy loss in red, gas detector signal in cyan, and Gaussian fit to the energy loss values in blue with a peak loss of 6.09 mJ.

An absolute thermal and single-shot thermo-acoustic X-ray pulse energy measurement [12] is being commissioned in a X-ray diagnostic chamber adjacent to the main beam dump to provide an independent absolute measurement of the photon pulse energy.

Configuration Changes

Changes of the LCLS machine configuration occur frequently when beam delivery switches to a different user experiment but are also common during an experiment's shift.

A fast change is the photon pulse length with the accessible range for soft x-rays from $60 - 500$ fs (FWHM) shown in Fig. 14. The X-ray pulse duration is only estimated based on the electron bunch length and is $60 - 100$ fs (FWHM) for hard X-rays. The electron bunch length is changed by phase settings in the L2 linac to change the chirp into the second bunch compressor. This changes the energy profile in the L2 linac and in order to get maximum FEL pulse energy requires a scaling of the magnets which takes about one minute for each data point in the figure.

The setting of the photon energy is done via the electron beam energy. A small change up to 10s of MeV can be immediately set with an energy offset in the longitudinal feedback for the L3 linac and does not change any magnet settings. For medium changes of a few GeV an auto-

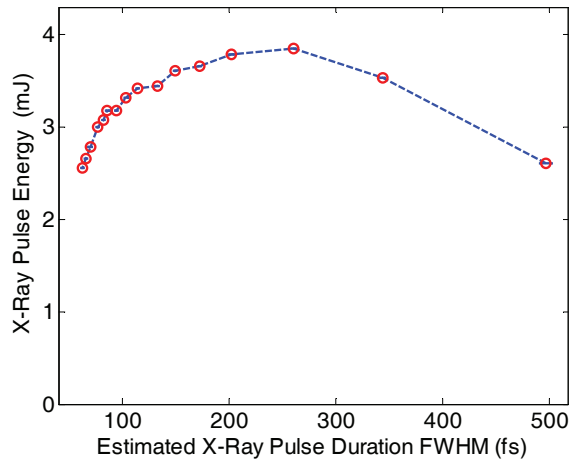

Figure 14: Tuning range of the estimated X-ray pulse length for soft X-rays. The corresponding peak power reaches above 40 GW (hard X-rays 75 GW).

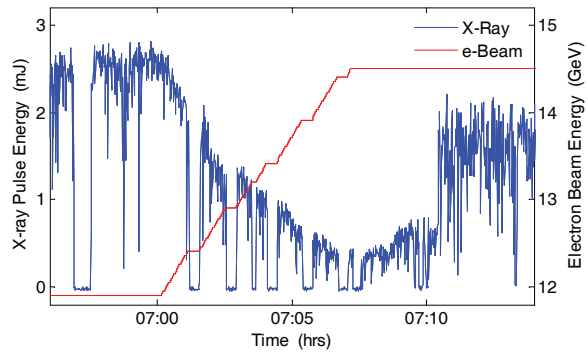

Figure 15: X-ray pulse energy during energy ramp from about 12 to 14.5 GeV. The jump in photon energy around 7:10 is due the recalibration of the gas detector.

mated script [13] increases or decreases the main energy set point for the energy feedback and continuously scales all necessary magnets to the new beam energy while the energy feedback adjusts the RF phases accordingly. Every 250 MeV the software adds to or drops from the accelerating complement one station. An example of the procedure is shown in Fig. 15 with an energy change from 12 to 14.5 GeV which took about 10 min and resulted in a reduction of the X-ray pulse energy of 30% without any further tuning of the machine.

SUMMARY

Over the last two years since user operation started the LCLS has reliably delivered soft and hard X-ray beams to a growing number of user experiments. The presently available parameter range far exceeds the original design and is used to its full extend by the LCLS users. A large number of feedback systems supports stable X-ray beam operation and matured software applications enable fast changes of

ISBN 978-3-95450-117-5

the machine configuration and aide machine setup and optimization.

ACKNOWLEDGEMENTS

The author wishes to thank all the coworkers in the LCLS commissioning team and the colleagues from ANL and LLNL for their many contributions.

REFERENCES

[1] J. Arthur, *et al.*, Linac Coherent Light Source (LCLS) conceptual design report, SLAC-R-593, SLAC (2002).

[2] P. Emma, *et al.*, Nature Photon. 4 (2010) 641.

[3] H. Loos, *et al.*, Proceedings of BIW 2010, Santa Fe, NM, May 2010, p. MOIANB01 (2010).

[4] Y. Ding, *et al.*, Phys. Rev. Lett. 102 (2009) 254801.

[5] R. Akre, *et al.*, Phys. Rev. ST Accel. Beams 11 (2008) 030703.

[6] J. Wu, *et al.*, Proceedings of FEL 2008, Gyeongju, Korea, Aug. 2008, p. MOPPH052 (2008).

[7] D. Fairley, *et al.*, Proceedings of ICALEPCS 2009, Kobe, Japan, Oct. 2009, p. THB001 (2009).

[8] P. Emma, *et al.*, Nucl. Instr. and Meth. A 429 (1999) 407.

[9] H.-D. Nuhn, *et al.*, these proceedings, p. WEPB04 (2011).

[10] H.-D. Nuhn, Proceedings of FEL 2009, Liverpool, UK, Aug. 2009, p. THOA02 (2009).

[11] D. Ratner, *et al.*, Proceedings of FEL 2009, Liverpool, UK, Aug. 2009, p. THOA03 (2009).

[12] T. Smith, *et al.*, these proceedings, p. WEPA02 (2011).

[13] N. Lipkowitz, *et al.*, Proceedings of PAC 2011, New York, NY, March 2011, p. WEOBS4 (2011).

ISBN 978-3-95450-117-5